



Contents lists available at ScienceDirect

International Journal of Mass Spectrometry

journal homepage: www.elsevier.com/locate/ijms



Theoretical study of electron capture dissociation of $[\text{Mg}(\text{H}_2\text{O})_n]^{2+}$ clusters

Diane Neff, Jack Simons*

Chemistry Department and Henry Eyring Center for Theoretical Chemistry, University of Utah, Salt Lake City, UT 84112, United States

ARTICLE INFO

Article history:

Received 26 March 2008
Received in revised form 13 May 2008
Accepted 15 May 2008
Available online xxx

Keywords:

Electron capture dissociation
Dissociative attachment
Water clusters

ABSTRACT

The electron capture dissociation (ECD) of $[\text{Mg}(\text{H}_2\text{O})_n]^{2+}$ clusters is examined using ab initio electronic structure methods to interpret experimental data on $[\text{Mg}(\text{H}_2\text{O})_n]^{2+}$ and $[\text{Ca}(\text{H}_2\text{O})_n]^{2+}$. Calculations are performed on $\text{Mg}^{2+}(\text{H}_2\text{O})_n$ clusters containing a full first hydration shell plus one or two additional water molecules positioned to represent second- and third-shell molecules. The propensity of the Mg-containing clusters to undergo fragmentation primarily into $[\text{Mg}(\text{H}_2\text{O})_{n-m}]^{1+} + m \text{H}_2\text{O}$ ($m = 10$) for $n > 17$ but primarily into $[\text{Mg}(\text{OH})(\text{H}_2\text{O})_{n-k}]^{1+} + \text{H} + (k-1) \text{H}_2\text{O}$ ($k-1 = 10$) for $n < 17$ (for Ca-containing clusters, the transition occurs near $n = 22$) is rationalized in terms of a model in which:

- For Mg with $n < 17$ (< 22 for Ca), the second hydration shell is not filled, so electron attachment can occur either directly into an O–H σ^* orbital of a first-shell water molecule or into a Rydberg orbital surrounding the cluster, after which electron transfer to a first-shell O–H σ^* orbital occurs, liberating an H atom and generating OH^- . The experimental observation that 10 water molecules are released is shown to favor a mechanism in which electron attachment to a Rydberg orbital occurs first and is followed by transfer to an O–H σ^* orbital.
- For Mg with $n > 17$, the second hydration shell is posited to be filled, and it is shown that electron attachment to a second-shell water O–H σ^* orbital is unlikely. So, electron attachment to a surface-localized Rydberg orbital of the $[\text{Mg}(\text{H}_2\text{O})_n]^{2+}$ cluster takes place in a 5-eV exothermic process that boils off ca. 10 water molecules. No $\text{OH}^- + \text{H}$ is formed in such cases.

© 2008 Elsevier B.V. All rights reserved.

1. Introduction

Electron capture dissociation (ECD) experiments have been carried out [1] on doubly charged water-cluster cations $\text{M}(\text{H}_2\text{O})_n^{2+}$, where M is an alkaline earth atom. In these experiments, mass-selected doubly charged cations $\text{M}(\text{H}_2\text{O})_n^{2+}$ are subjected to ECD after which the mass-to-charge ratios and abundances of the fragment ions are determined. For clusters containing $> \text{ca. } 20$ water molecules, workers observed [1] the loss of 10 ± 1 H_2O molecules upon electron capture, regardless of whether the metal M was Mg, Ca, Sr, or Ba. In Fig. 1, we show a table from Ref. [1b] illustrating these findings on parent species containing 32 water molecules.

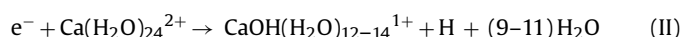
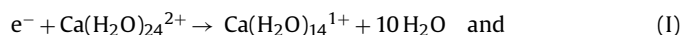
The fact that the same number (10) of water molecules are lost regardless of which metal dication is present suggests that the ECD electron is not captured at the M^{2+} dication to generate a M^{1+} cation. The $\text{e}^- + \text{M}^{2+} \rightarrow \text{M}^{1+}$ recombination energies of these bare dications

vary from 15 eV (for Mg) to 10 eV (for Ba), so one would expect the number of water molecules lost to vary considerably if the metal dication were being reduced in the ECD process and the energy thus released were converted to vibrational energy which then caused water molecules to be ejected.

Moreover, in Ref. [1] it was shown that ca. 10 kcal mol^{-1} is needed to “boil off” each H_2O molecule in this size range, so the fact that 10 ± 1 water molecules are lost is interpreted to suggest that the approximately $100 \text{ kcal mol}^{-1}$ released upon electron capture by $\text{M}(\text{H}_2\text{O})_n^{2+}$ cations in this size range is quickly randomized within the internal degrees of freedom of the cluster and fully utilized to boil off water molecules.

However, when examining the nature and abundances of the ECD product ions as functions of cluster size (n), an interesting result was found [1a] as illustrated in Fig. 2 for $\text{Ca}(\text{H}_2\text{O})_{24}^{2+}$.

There seems to be two fragmentation paths both of which involve boiling off water molecules,



one ejecting 10 water molecules and the second involving conversion of one water molecule to hydroxide OH^- and a hydrogen atom

* Corresponding author. Tel.: +1 801 581 8023.
E-mail address: simons@chem.utah.edu (J. Simons).
URL: <http://simons.hec.utah.edu> (J. Simons).

$M(\text{H}_2\text{O})_{32}^{2+}$	Number of Molecules Lost			Weighted Average	
	-11	-10	-9	ECD	corrected
Mg	61	100	<9	10.4	10.3
Ca	30	100	<7	10.2	10.2
Sr	34	100	20	10.1	10.0
Ba	25	100	<10	10.2	10.1

Fig. 1. Data taken from Ref. [1b] showing that 10 ± 1 water molecules are lost from doubly charged alkaline metal cluster cations upon ECD.

while also boiling off 9–11 water molecules. When the products of ECD experiments on calcium-containing clusters containing 4–47 water molecules were probed, the fraction of H-atom loss accompanied by water loss (pathway II) changed sharply from near 100% for $n < 22$ to near 0% for $n > 30$ as shown in Fig. 3.

Similar trends in the branching ratios for $[\text{Mg}(\text{H}_2\text{O})_n]^{1+}$ clusters fragmenting into either $[\text{Mg}(\text{H}_2\text{O})_{n-m}]^{1+} + m \text{H}_2\text{O}$ or $[\text{Mg}(\text{OH})(\text{H}_2\text{O})_{n-k}]^{1+} + \text{H} + (k-1) \text{H}_2\text{O}$ have been observed [2] by earlier workers not under ECD conditions but using laser vaporization of Mg powder in the presence of water vapor as well as other techniques [3,4]. For the Mg-containing clusters, the transition from dominance of H atom loss to water loss seems to begin at around $n = 17$ rather than near $n = 22$ as found for Ca-containing clusters.

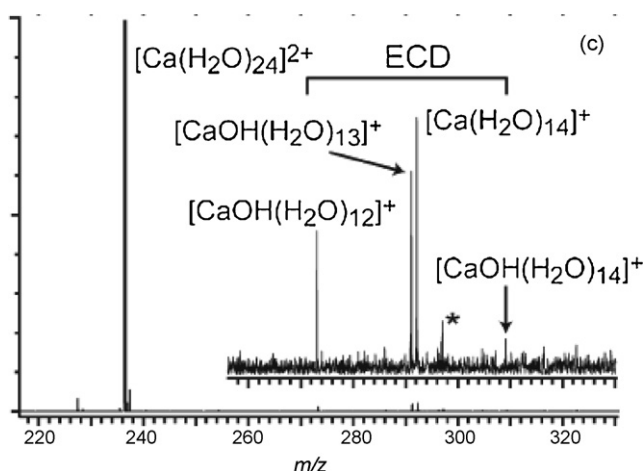


Fig. 2. Mass spectrum of ECD products resulting from ECD of $\text{Ca}(\text{H}_2\text{O})_{24}^{2+}$ showing mono-cations $\text{Ca}(\text{H}_2\text{O})_{14}^{1+}$ produced from water loss and species $\text{CaOH}(\text{H}_2\text{O})_{12-14}^{1+}$ containing the CaOH unit (from Ref. [1a]).

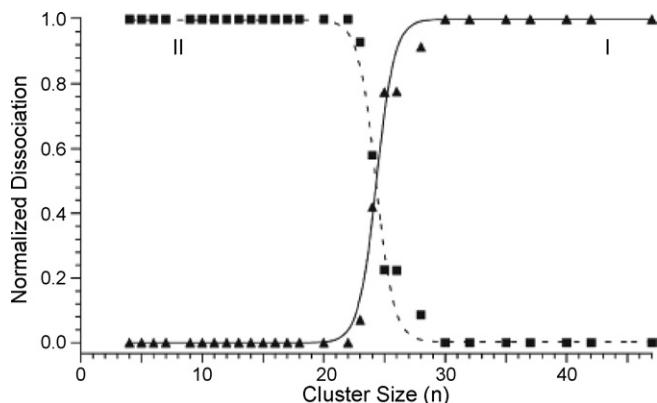


Fig. 3. Fraction of water loss (I) and H-atom loss (II) for $\text{Ca}(\text{H}_2\text{O})_n^{2+}$ (from Ref. [1a]).

To us, these findings on the charge-separation reactions of $\text{M}(\text{H}_2\text{O})_n^{2+}$ complexes suggest that in the ECD studies of the competition occurring in, for example, $\text{e}^- + \text{Ca}(\text{H}_2\text{O})_{24}^{2+} \rightarrow \text{Ca}(\text{H}_2\text{O})_{14}^{1+} + 10 \text{H}_2\text{O}$ and $\text{e}^- + \text{Ca}(\text{H}_2\text{O})_{24}^{2+} \rightarrow \text{CaOH}(\text{H}_2\text{O})_{12-14}^{1+} + \text{H} + 9-11 \text{H}_2\text{O}$, the H-atom loss could occur either by

1. attachment of an electron to $\text{Ca}(\text{H}_2\text{O})_{24}^{2+}$ releasing the 4.5–5 eV recombination energy into internal vibrational modes of the nascent $\text{Ca}(\text{H}_2\text{O})_{24}^{1+}$ that either
 - a. causes loss of 10 water molecules to produce $\text{Ca}(\text{H}_2\text{O})_{14}^{1+}$, or
 - b. provides a water molecule in the inner hydration shell enough energy to dissociate into OH^- and a proton that is transferred outward (i.e., perhaps in a Grotthuss-like mechanism) to a water molecule in an outer hydration shell to generate H_3O^+ (and liberate 9–11 water molecules). Subsequently, the H_3O^+ could pick up the ECD-attached electron residing on the surface of the cluster to generate neutral H_3O (which we know [5] falls apart to produce $\text{H} + \text{H}_2\text{O}$), or
2. attachment of an electron directly to a Coulomb-stabilized σ^* orbital of a water molecule (likely one near or on the surface of the $\text{Ca}(\text{H}_2\text{O})_{24}^{2+}$ cluster) to promptly liberate an H atom, boil off 9–11 water molecules, and generate a surface OH^- anion that subsequently abstracts a proton from a nearby H_2O molecule allowing the OH^- charge center to propagate inward toward the M^{2+} center to generate $\text{CaOH}(\text{H}_2\text{O})_{12-14}^{1+}$.

Either of these two mechanistic possibilities could produce $\text{MOH}(\text{H}_2\text{O})_{n-k-1}^{1+} + \text{H} + (n-k) \text{H}_2\text{O}$ from $\text{M}(\text{H}_2\text{O})_n^{2+}$, and it is the purpose of this work to try to determine how this $\text{OH}^- + \text{H}$ generation is taking place.

Our suggestion that an ECD electron could attach directly to a water molecule's $\text{OH} \sigma^*$ orbital derives from our ongoing work [6] aimed at understanding the mechanisms by which peptide and protein disulfide and $\text{N}-\text{C}_\alpha$ bonds are cleaved under ECD conditions. The basic idea is that the energy of an electron-attached state can be lowered by the Coulomb potential of any nearby positively charged site. This Coulomb energy C in eV can be expressed in terms of the distance R in Å between the positive site of charge Q and the electron-attached site as

$$C \text{ (eV)} = 14.4 \frac{Q}{R} \quad (1)$$

In the present work, we consider the possibility that the Coulomb stabilization can render exothermic the attachment of an electron to a water molecule's $\text{OH} \sigma^*$ orbital. In particular, we examine the energy profiles of doubly charged $\text{Mg}^{2+}(\text{H}_2\text{O})_n$ and of the same species [7] with an electron attached to an $\text{OH} \sigma^*$ orbital belonging to one of the water molecules. For small n , this water resides in the first or second hydration layer; for larger n , it resides in the third layer.

To see why we raise the possibility of Coulomb-assisted attachment to an $\text{OH} \sigma^*$ orbital, let us again examine the data shown in Fig. 3. Note that the prevalence of the charge-exchange reaction over the pure water-loss reaction changes sharply over a narrow range of cluster size. For clusters $\text{Ca}(\text{H}_2\text{O})_n^{2+}$ having $n < 22$, one observes only charge exchange plus loss of 10 water molecules; essentially no loss of 10 water molecules without charge exchange occurs for $n < 22$. To us, this suggests that, for $n < 22$, the surface H_2O molecules might be close enough to the Ca^{2+} charge to render exothermic Coulomb-assisted electron attachment to the surface waters' $\text{O}-\text{H} \sigma^*$ orbitals, whereas, for $n > 30$, the distance from the Ca^{2+} center to the surface H_2O molecules may be too large to sufficiently Coulomb-stabilize these water $\text{O}-\text{H} \sigma^*$ orbitals. This hypothesis is what we address in the present work.

2. Methods

Based on our success in simulating peptide fragmentation events, we decided to perform our calculations at the unrestricted second-order Møller–Plesset (UMP2) level of theory using one set (1s1p) of extra-diffuse basis functions [8] centered on the positive sites' central atom as well as aug-cc-pVDZ basis sets [9] on all atoms. Because the methods we used are based on unrestricted wave functions, it is important to make sure that little artificial spin contamination enters into the final wave functions. We computed (S^2) for species studied in this work and found values not exceeding (before annihilation) the expected value of $S(S+1)=0.75$ by more than 0.01 for the Rydberg-attached and σ^* -attached doublets. For the parent $[\text{Mg}(\text{H}_2\text{O})_n]^{2+}$ clusters, as expected, the highest spin contamination $S(S+1)=0.95$ occurred near asymptotes where an O–H bond is homolytically cleaved; at O–H bond lengths where curve crossings important in this study occurred, the spin contamination was much less.

In all of the calculations discussed below, the geometries used were obtained as follows:

1. For the parent $[\text{Mg}(\text{H}_2\text{O})_n]^{2+}$ clusters, the geometry was first optimized at the UHF level and then at the UMP2 level. When one of the O–H bonds was elongated, all of the other geometrical degrees of freedom were relaxed (at the UMP2 level), except for the constraints noted below relating to how we orient the outermost water molecules in clusters with second- or third-shell waters.
2. For the charge-reduced $[\text{Mg}(\text{H}_2\text{O})_n]^{1+}$ clusters with an electron attached to a surface Rydberg orbital, the geometry of the parent $[\text{Mg}(\text{H}_2\text{O})_n]^{2+}$ was used. This was done to allow us to determine the energy gained upon vertical attachment of an electron to $[\text{Mg}(\text{H}_2\text{O})_n]^{2+}$.
3. For the charge-reduced $[\text{Mg}(\text{H}_2\text{O})_n]^{1+}$ clusters with an electron attached to an O–H σ^* orbital, two sets of calculations were performed:
 - a. In one set, the geometry of the parent $[\text{Mg}(\text{H}_2\text{O})_n]^{2+}$ was used, again to allow us to consider vertical electron attachment.
 - b. In the second set, for each value of the elongated O–H bond length, the other geometrical degrees of freedom were relaxed. These data allowed us to explore how much additional energy is released as the O–H bond fragments and the cluster's geometry relaxes.

Difficulties arise when carrying out computations of the O–H σ^* electron-attached state at each O–H bond length, especially when the energy of this state is above that of the parent system. Under these circumstances, electron detachment can occur as variational collapse to the energy of the parent plus a free (i.e., continuum) electron takes place. In such cases, we had to use an approach that we have employed in many past applications [10] to obtain the energy of this metastable electronic state. Specifically, we artificially increased by a small amount δq the nuclear charges of the atoms (the oxygen and hydrogen atoms forming the O–H σ^* state) involved in accepting the transferred electron, and carried out the UMP2 calculations with these artificial nuclear charges. By plotting the energies of the O–H σ^* state relative to that of the parent species for several values of the charge increment δq and extrapolating to $\delta q=0$, we were able to obtain our approximations to the true energies of these metastable states.

Finally, we note that all calculations were performed using the Gaussian 03 suite of programs [11], and the three-dimensional plots of the molecular orbitals were generated with the MOLDEN program [12].

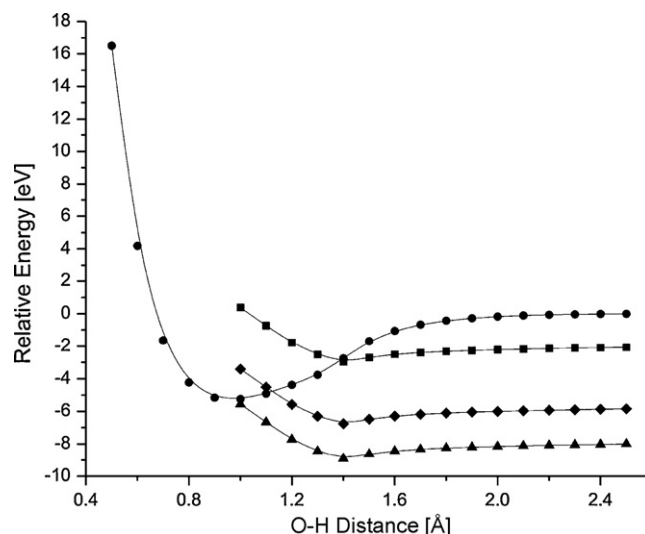


Fig. 4. MP2-level energies of neutral water (circles) and of H_2O^- (squares) in which the excess electron resides in the σ^* orbital of the OH bond being stretched. Also shown are the MP2 energies expected on the basis of Coulomb stabilization for the H_2O^- species in the presence of a Mg^{2+} cation at distances from the H_2O representative of the second (triangles) and third (diamonds) hydration shells of $\text{Mg}^{2+}(\text{H}_2\text{O})_n$.

3. Results

3.1. Building blocks: electron attachment to water or to $\text{Mg}(\text{H}_2\text{O})_6^{2+}$

The first set of results we display relate to the fragments upon which we base this study: Mg^{2+} , $\text{Mg}(\text{H}_2\text{O})_n^{2+}$ clusters, and H_2O molecules. In Fig. 4, we show the energies of a single water molecule and of a water molecule with an electron attached to one of its OH σ^* orbitals as functions of the length of the OH bond within whose σ^* orbital the excess electron resides.

The lower two curves in Fig. 4 were obtained by shifting the upper H_2O^- curve downward by 6.1 eV and 3.8 eV [13], and thus they offer approximations to what we expect to find for attaching an electron to a second or third hydration shell water molecule in larger $\text{Mg}^{2+}(\text{H}_2\text{O})_n$ clusters based on the Coulomb stabilization model. Later in this paper, we present results from actual ab initio calculations on such clusters.

We should note that the electronic nature of the anion state whose energy is plotted in Fig. 4 is of the shape-resonance type having one electron bound to the ground-state of H_2O . Other workers [14] have examined electron–water collisions, focusing mainly on Feshbach states in which an excess electron binds to an excited electronic state of H_2O , but these studies have not produced energy profiles of the shape-resonance state's energy as functions of one O–H bond length as we needed here.

The main points to make about the data in Fig. 4 are:

1. It is substantially endothermic to vertically attach an electron to H_2O in the absence of Coulomb stabilization. This means that an ECD electron will not attach to an OH σ^* orbital of a neutral water molecule in the absence of other influences because these electrons do not have sufficient kinetic energy.
2. The OH bond length would have to be extended to ca. 1.4 Å (prior to electron attachment) to render σ^* orbital attachment to neutral H_2O feasible in the absence of the Coulomb potential. To access such a long OH bond length through vibrational motion, the temperature would have to be much higher than in ECD experiments.

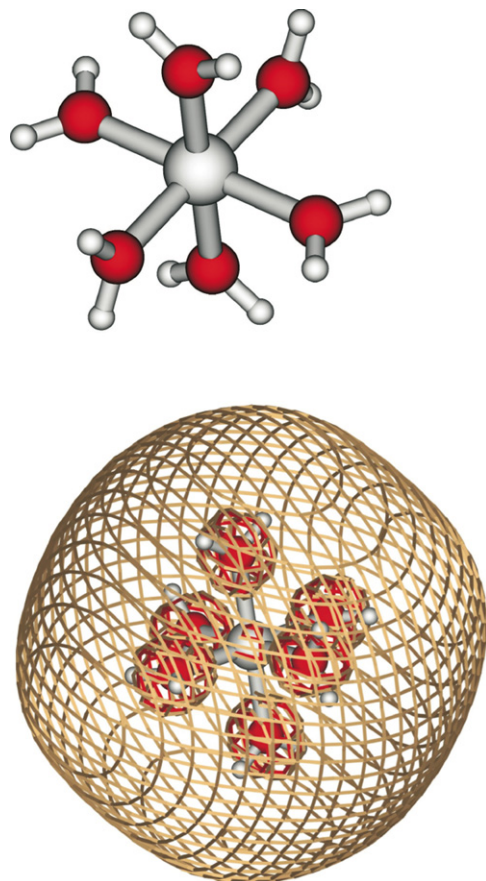


Fig. 5. MP2-level minimum-energy structure of $\text{Mg}^{2+}(\text{H}_2\text{O})_6$ (top) in which the Mg–O distance is 2.1 Å, and surface-localized orbital to which an electron binds to form $[\text{Mg}(\text{H}_2\text{O})_6]^+$ (bottom).

3. With a Coulomb potential representative of that experienced by water molecules in the second hydration layer in $\text{Mg}^{2+}(\text{H}_2\text{O})_n$, vertical electron attachment to an OH σ^* orbital might be exothermic.
4. With a Coulomb potential representative of that experienced by the third hydration layer in $\text{Mg}^{2+}(\text{H}_2\text{O})_n$, vertical electron attachment to an OH σ^* orbital is endothermic by ca. 0.3 eV.
5. Once an electron attaches to an OH σ^* orbital, fragmentation to form OH^- and H is prompt because the σ^* potential surface is repulsive.

These data offer the first suggestions about can be expected for $\text{Mg}^{2+}(\text{H}_2\text{O})_n$ clusters.

However, there is another electron-attached state whose energy profile is not shown in Fig. 4, and this state can compete with the O–H σ^* attachment processes just discussed. In Fig. 5, we show the optimized structure obtained for the $\text{Mg}^{2+}(\text{H}_2\text{O})_6$ cluster we employ to model the first solvation shell of Mg^{2+} as well as the lowest-energy Rydberg orbital formed when this cluster binds an excess electron. Such surface-localized states have been suggested as being involved in $[\text{Mg}(\text{H}_2\text{O})_n]^{1+}$ clusters by several earlier workers who have considered the stabilities of $[\text{Mg}(\text{H}_2\text{O})_n]^{1+}$ clusters [15–22]. In such a “surface-state” Rydberg orbital, the electron is bound by ca. 5 eV [23], and it is attachment to this orbital that can compete with O–H σ^* attachment. We note that the 5 eV binding energy is in line with what was inferred [1a,1b] from experimental data [24], and that the optimized Mg–O distance (2.1 Å) in $\text{Mg}^{2+}(\text{H}_2\text{O})_6$ is similar to what was found [25] other workers’ earlier calculation on such species.

Now, let us combine the knowledge presented above to anticipate what is likely to happen when an electron binds to a $[\text{Mg}(\text{H}_2\text{O})_n]^{2+}$ cluster containing more than six water molecules. For clusters in which the first hydration shell is filled (i.e., $n > 6$) but with the second hydration shell not completely filled, we expect either of two things to happen when an electron attaches:

1. The electron can attach to a surface-localized Rydberg orbital of the cluster (in a 5-eV exothermic process) to form a charge-reduced species $[\text{Mg}(\text{H}_2\text{O})_6]^+ (\text{H}_2\text{O})_{n-6}$ containing $n-6$ water molecules outside the first hydration layer, or
2. The electron might attach to an O–H σ^* orbital of a water molecule residing in the second hydration shell generating $[\text{Mg}(\text{H}_2\text{O})_6]^{2+} (\text{OH}^-) (\text{H}_2\text{O})_{n-7} + \text{H}$. As we show later, this process is 4 eV exothermic and releases an H atom.

In either of these two processes, the considerable exothermicity would be expected to also boil off up to water molecules. The data of Fig. 4 suggest that a water molecule residing at a distance outside the second hydration shell is unlikely to attach an electron.

3.2. The $[\text{Mg}(\text{H}_2\text{O})_6]^{2+} \text{H}_2\text{O}$ and $[\text{Mg}(\text{H}_2\text{O})_6]^{2+} (\text{H}_2\text{O})_2$ model systems

We next had to construct two model systems in which we explored what happens when an electron attaches to an O–H σ^* orbital of a water molecule occupying a site on either the second or third hydration shell of a $\text{Mg}^{2+}(\text{H}_2\text{O})_n$ cluster.

To form a representation of a cluster with one water molecule outside two hydration shells, we would have to first determine how many molecules constitute the second-shell and then add one more. To the best of our knowledge, it is not known with much certainty how many water molecules lie in the second-shell (for either Mg^{2+} or Ca^{2+}). Moreover, it would be extremely computationally difficult to perform the kind of calculations used in this work on such a large cluster. For these reasons, we chose to model the behavior of a water molecule residing within the third hydration shell using the second model species shown in Fig. 6.

To construct this $\text{Mg}^{2+}(\text{H}_2\text{O})_8$ cluster, we constrained the oxygen atoms of the two water molecules’ outside the first hydration shell to lie on a line connecting the Mg^{2+} ion to an oxygen atom of one of the six water molecules in the first hydration layer. If we do not so constrain the outer two water molecules, geometry optimization leads to a structure with the outer two molecules in the second hydration shell, thereby defeating our strategy of having one water molecule in the second-shell and another at a distance characteristic of the third shell.

With this constraint in place, we optimized the geometries of model systems containing seven or eight water molecules. We obtained the structure described in Fig. 6 for the $\text{Mg}^{2+}(\text{H}_2\text{O})_6 (\text{H}_2\text{O})_2$ case; the optimized structure of $\text{Mg}^{2+}(\text{H}_2\text{O})_6 (\text{H}_2\text{O})_1$ was essentially identical except for the third-shell water.

The first thing to note about the structures of these model systems is that the Mg–O distance associated with the first hydration shell are essentially the same as we found (Fig. 5) for $\text{Mg}^{2+}(\text{H}_2\text{O})_6$. This means that the presence of the (model) second- and third-shell water molecules does not qualitatively alter the structure of the first-shell. Of course, we cannot with certainty conclude that the locations of the inner six water molecules relative to the Mg^{2+} ion will remain so unchanged as more water molecules are added to the second-shell, but these data suggest that changes will likely be small. Also, the O–O distances in the seven and eight water model compounds (2.6–2.9 Å) are similar to the O–O distance in the water dimer (2.98 Å).

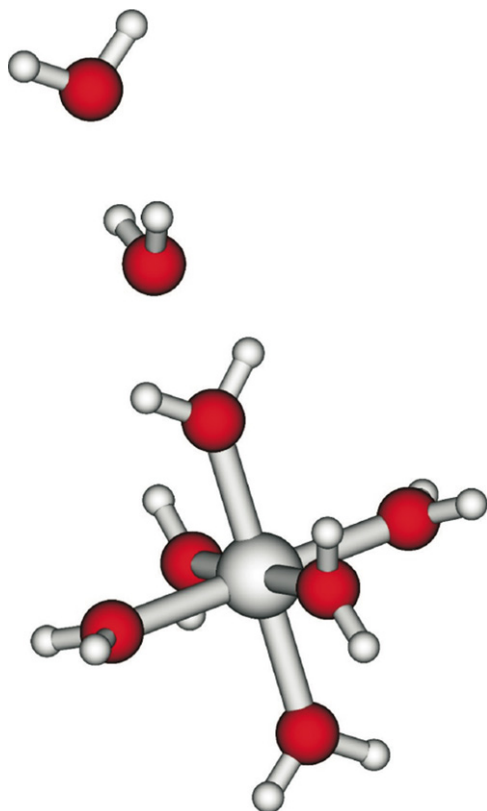


Fig. 6. $\text{Mg}^{2+}(\text{H}_2\text{O})_6 (\text{H}_2\text{O})_2$ structure used to model one full hydration shell with two water molecules occupying distances characteristic of second and third shells. The Mg–O distances are 2.1 Å, 4.7 Å, and 7.6 Å for the first-, second-, and third-shell water molecules, respectively. In the seven-water cluster, the respective distances are 2.1 Å and 4.8 Å.

3.3. The surface Rydberg and O–H σ^* orbitals

In Fig. 7, we show the surface-localized Rydberg orbitals for the $\text{Mg}^+(\text{H}_2\text{O})_6 (\text{H}_2\text{O})_1$ and $\text{Mg}^+(\text{H}_2\text{O})_6 (\text{H}_2\text{O})_2$ model systems.

These orbitals look much like the Rydberg orbital of the $\text{Mg}^+(\text{H}_2\text{O})_6$ cluster shown in Fig. 5. Moreover, the strength with which they bind the excess electron (5 eV) is also essentially the same as in the $\text{Mg}^+(\text{H}_2\text{O})_6$ case and what others found earlier for larger $[\text{Mg}(\text{H}_2\text{O})_n]^{1+}$ clusters [26]. Note that these orbitals have most of their density in regions near the first-shell water molecules

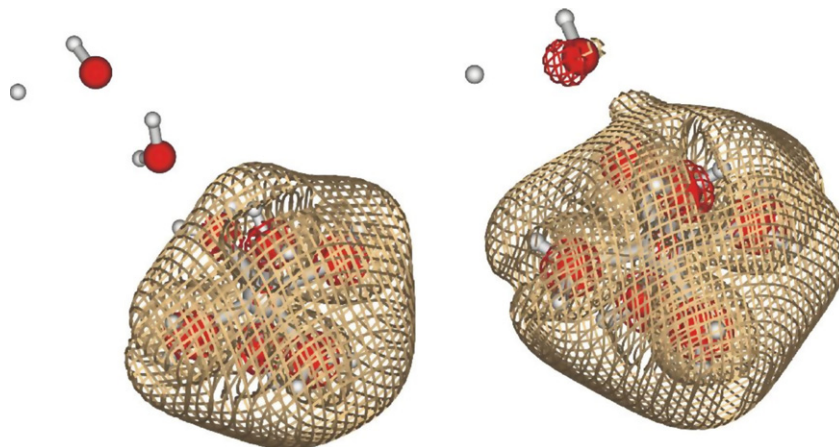


Fig. 7. Surface Rydberg orbitals of $\text{Mg}^{2+}(\text{H}_2\text{O})_n$ containing seven (right) or eight (left) water molecules.

where they can experience the most attraction from the Mg^{2+} ion's potential.

In Fig. 8, the relaxed geometries of the parent $\text{Mg}^{2+}(\text{H}_2\text{O})_6 (\text{H}_2\text{O})_1$ and $\text{Mg}^{2+}(\text{H}_2\text{O})_6 (\text{H}_2\text{O})_2$ species are shown (top) as well as the relaxed geometries (bottom) of the corresponding species in which an electron is attached to an O–H σ^* orbital on the outermost water molecule for one value of the elongated O–H bond length. In addition, Fig. 8 displays the O–H σ^* orbitals for these states.

In the bottom pictures, the antibonding character of the O–H orbital is clearly shown. Even after the geometries are allowed to relax, the Mg–O distances within the inner hydration shell do not differ significantly from those in the bare $\text{Mg}^{2+}(\text{H}_2\text{O})_6$ or in the surface-bound state of $\text{Mg}^+(\text{H}_2\text{O})_6$.

3.4. Energy profiles of parent and electron-attached species

In Fig. 9, we display the energy profiles, as functions of the elongated O–H bond length on the outermost water molecule, for $\text{Mg}^{2+}(\text{H}_2\text{O})_6 (\text{H}_2\text{O})_1$ and $\text{Mg}^{2+}(\text{H}_2\text{O})_6 (\text{H}_2\text{O})_2$ as well as for states with an electron attached either to the surface-localized Rydberg orbital or to an O–H σ^* orbital of the outermost water molecule. For the σ^* -attached states, we show data pertinent to vertical electron attachment at the parent's optimized geometry and for attachment into this σ^* orbital after which the charge-reduced cluster's geometry is allowed to “relax” to become optimal for this charge state. The former allows us to draw conclusions about whether an electron can exothermically attach when the cluster is at a geometry near that of the parent. The latter tells us how much additional energy is released once an electron is attached and the charge-reduced species relaxes.

The first thing to notice in Fig. 9 is, for both model clusters, the Rydberg-attached state's energy profile parallels that of the parent and lies 5 eV below the parent, as expected from our earlier findings. This suggests that electron attachment to a cluster that has most of its first hydration shell accessible (i.e., with not many water molecules occupying sites in the second-shell) can be expected to generate a surface-bound Rydberg state [15] and to liberate 5 eV, which can, in turn, boil off 10 water molecules. The next thing to notice is that the σ^* -attached state's curves are similar to what the simple Coulomb model reflected in Fig. 4 suggested.

The data shown in Fig. 9 also suggest that, near O–H bond lengths accessible by zero-point vibrational motion prior to electron attachment, direct attachment to an O–H σ^* orbital of a second-shell water molecule *might* be feasible because the neutral and unrelaxed anion's curves intersect near the minimum of the

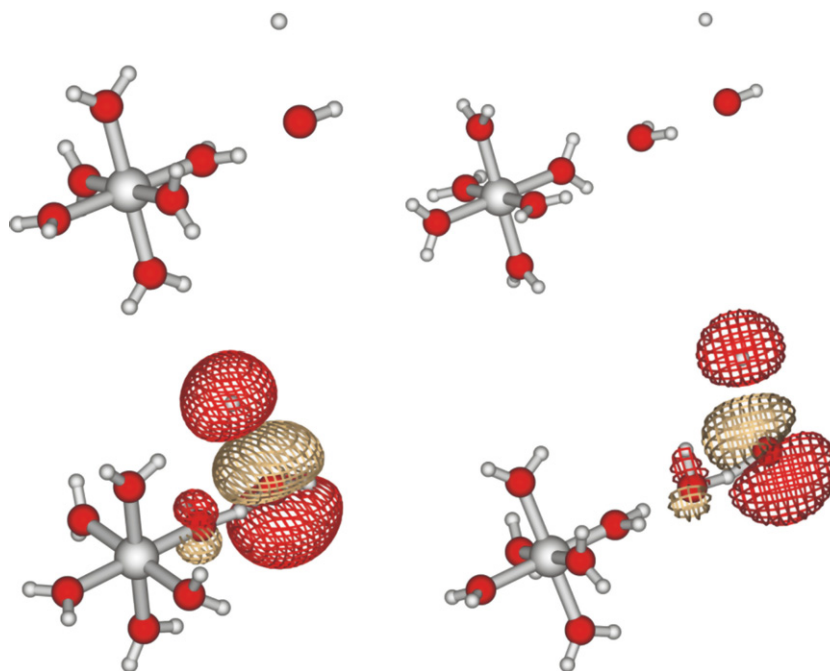


Fig. 8. Relaxed geometries of dications containing seven or eight water molecules (top) and of species with electron attached to O–H σ^* orbital of outermost water molecule, with this orbital shown (bottom).

neutral. However, attachment to a σ^* orbital of a third-shell water molecule is not because the neutral and unrelaxed anion curves intersect far above the neutral's minimum.

One more conclusion can be drawn from Fig. 9 for the case of clusters having partially filled second hydration shells. Specifically, if an electron were captured into the surface-localized Rydberg orbital, it is unlikely to subsequently be transferred from this orbital into an O–H σ^* orbital of one of the second-shell water molecules. The electron would attach to the Rydberg orbital at O–H bond lengths that are thermally accessible (i.e., near 1 Å). To undergo transfer to a second-shell O–H σ^* orbital, the O–H bond length would have to elongate to near 1.5 Å, where the σ^* -attached and Rydberg-attached curves cross. To access such a bond length, the cluster would have to retain within its O–H stretching coordinate ca. 2 eV of the 5 eV released in the electron capture event, which would be highly improbable.

In summary, the formation of $[\text{Mg}(\text{H}_2\text{O})_6]^{2+}(\text{OH}^-)(\text{H}_2\text{O})_{n-7} + \text{H}$ from clusters with partially filled second shells would be expected to arise from the direct attachment of ECD electrons to second-shell O–H σ^* orbitals, but only if O–H bond lengths at which the unrelaxed σ^* -attached and parent species surfaces intersect are accessible. Formation of $[\text{Mg}(\text{H}_2\text{O})_6]^{2+}(\text{OH}^-)(\text{H}_2\text{O})_{n-7} + \text{H}$ by first attaching to the surface Rydberg orbital and then undergoing electron transfer to a second-shell O–H σ^* orbital will not happen. However, to attach an electron to a second-shell O–H σ^* orbital requires there be ca. 0.3 eV in the O–H vibrational mode prior to electron attachment to access where the unrelaxed σ^* -attached and parent's curves cross. Under ECD conditions, accessing this crossing seems doubtful, so we are now lead to examine another possibility that a first-shell water molecule undergoes direct attachment into one of its O–H σ^* orbitals to generate the $\text{H} + \text{OH}^-$ units.

3.5. The role of first-shell O–H σ^* orbitals

In this component of our investigation, we attempted to simulate what happens when an ECD electron is captured by a

cluster containing a full first hydration shell plus additional water molecules, but not enough additional waters to complete the second hydration shell. Although we utilize a model containing only a full first hydration shell of six water molecules in these simulations, we view this study to be pertinent to clusters containing additional (i.e., second-shell) waters as long as (i) at least one first-shell water molecule is exposed (i.e., has one of its OH σ^* orbitals spatially exposed) to the incoming ECD electron and (ii) the cluster's surface is able to capture an electron into a surface-bound Rydberg orbital in a ca. 5 eV exothermic process [26].

We assume that the ECD electron can access either a surface-bound Rydberg orbital or one of the O–H σ^* orbitals of a first-shell water molecule, and we examine what can happen subsequent to either such capture event. In Fig. 10, we show energy profiles as functions of an O–H bond length of one of the first-shell water molecules. Profiles are shown for the parent $\text{Mg}^{2+}(\text{H}_2\text{O})_6$ as well as for species in which an attached electron resides in the Rydberg orbital and in which the excess electron resides in an O–H σ^* orbital of one of the first-shell water molecules [27]. Again, for the σ^* -attached state, both unrelaxed and relaxed energies are plotted.

The energy landscapes of Fig. 10 allow us to predict that:

- Vertical attachment into a first-shell water molecule's O–H σ^* orbital can take place because the unrelaxed σ^* -attached curve lies below that of the parent near the parent's equilibrium bond length.
- Subsequent to such a direct σ^* -attachment, an H atom will be liberated (promptly because of the repulsive nature of the σ^* surface) and up to 5 eV may be deposited into the charge-reduced $[\text{Mg}(\text{OH})(\text{H}_2\text{O})_5]^{1+}$ cluster ion thus boiling off as many as 10 second-shell water molecules. However, it is more likely, if this process occurs, that translationally hot H atoms will be ejected and fewer than 10 water molecules boiled off.
- Alternatively, an ECD electron can attach to a Rydberg orbital, releasing 5 eV, which, after energy randomization occurs, can boil off up to 10 second-shell water molecules.

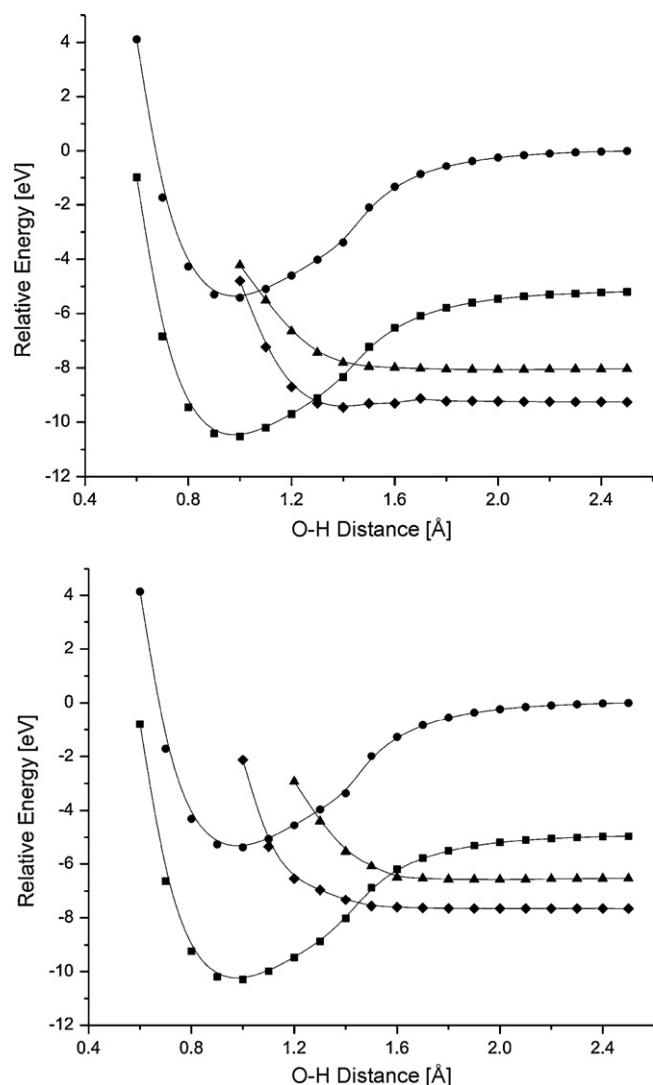


Fig. 9. MP2-energies of the parent dication (circles), Rydberg-attached (squares), unrelaxed σ^* -attached (triangles), and relaxed σ^* -attached (diamonds) states for clusters with seven (top) and eight (bottom) water molecules.

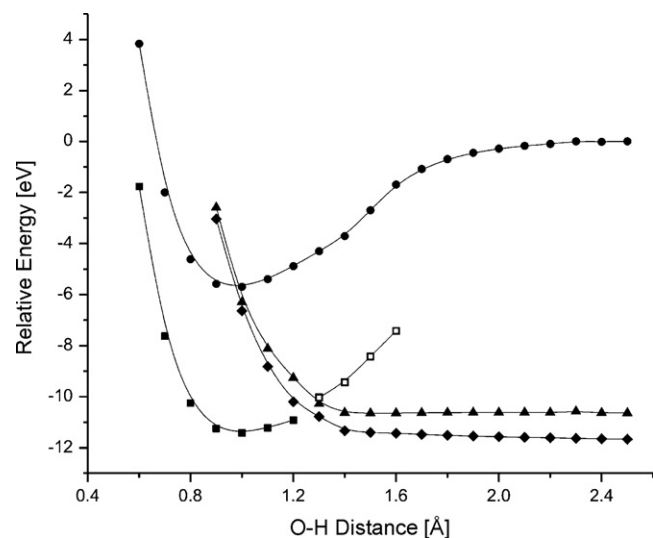


Fig. 10. MP2 energies of the parent dication (circles), surface Rydberg-attached (squares), unrelaxed σ^* -attached (triangles), and relaxed σ^* -attached (diamonds) states for the $[\text{Mg}(\text{H}_2\text{O})_6]^{2+}$ cluster. See [28] for explanation of open squares.

d. Finally, after an ECD electron attaches to a Rydberg orbital and the 5 eV exothermicity is randomized among the cluster's vibrational modes, the electron can subsequently transfer into an O–H σ^* orbital of one of the first-shell water molecules. This requires surmounting the small barrier where the Rydberg and relaxed [29] σ^* -attached curves cross near 1.3 Å in Fig. 10. After crossing (some tunneling is also possible) this barrier, the cluster will release an H atom and generate a charge-reduced cluster containing the OH^- unit. This cluster can retain enough internal energy to also boil off 10 water molecules.

4. Summary

Let us return now to discuss how the possibilities raised above can be consistent with, and thus help interpret, the data shown in Fig. 3. In particular, why is it that the channel producing an H atom and OH^- (and boiling off 10 water molecules) dominates for Mg^{2+} clusters with $n < 17$, while the channel that only boils off 10 water molecules dominates for $n > 17$? This same question can be asked for the Ca^{2+} clusters where the transition occurs [2] near $n = 22$. In our opinion, our simulations suggest that these trends can be explained as follows:

1. For Ca^{2+} clusters with $n > 30$ (or Mg^{2+} clusters with $n > \text{ca. } 17$), the second hydration shell is full. Direct attachment to a second-shell O–H σ^* orbital is probably not feasible, which explains why no H atom loss is observed. The only thing that can happen is attachment to a surface-localized Rydberg orbital followed by boiling off ca. 10 water molecules once the 5 eV exothermicity has been randomized. The same conclusion applied to Mg^{2+} clusters with $n > 17$.
2. For Ca^{2+} clusters with $6 < n < 22$ (or Mg^{2+} clusters with $6 < n < 17$), the second hydration shell is not full, so O–H σ^* orbitals of some of the first-shell water molecules are spatially exposed to the ECD electron. Therefore, it is possible that an ECD electron can be captured directly into a first-shell O–H σ^* orbital or into a Rydberg orbital. Although our simulations cannot evaluate the branching ratio between the latter two possibilities, the experimental data of Ref. [1] provide strongly suggestive guidance. In particular, if direct attachment to first-shell O–H σ^* orbitals were dominant, one would expect the number of water molecules boiled off when H and OH^- are formed to begin at 10 but to range to significantly smaller numbers because the H atom would carry away a substantial fraction of the 5 eV exothermicity in the form of kinetic energy.
3. In contrast, if attachment to a Rydberg orbital followed by electron transfer (after energy randomization) to a first-shell O–H σ^* orbital were dominant, then most of the 5 eV exothermicity would be retained in the cluster and available to boil off water molecules, and one should thus observe mostly 10 water molecules being ejected. Indeed, the latter outcome is what is seen when OH^- and H are formed, so this means it is most likely that the initial ECD electron capture event occurs into a surface Rydberg orbital and that H + OH^- formation involves electron transfer from the Rydberg orbital to an O–H σ^* orbital.

These mechanistic proposals are similar to one offered earlier (e.g., see Fig. 7 in Ref. [2]) by others who studied water loss in $[\text{Mg}(\text{H}_2\text{O})_n]^{1+}$ clusters formed under different conditions than those arising in Ref. [1]. The features contained in our proposals that are new include (i) the idea that an ECD electron may attach directly to an O–H σ^* orbital and (ii) the suggestion that electron transfer from the surface Rydberg orbital to a first-shell O–H σ^* orbital is probably a key event in forming H and OH^- .

Finally, it may be useful to reflect on the circumstances under which one expects to observe phenomena similar to those studied here. First, to have direct attachment to an antibonding orbital of the ligand (i.e., H_2O in our case), the electron affinity (EA in eV) of the ligand fragment (OH) plus the Coulomb stabilization C of this EA from the metal ion having charge Q ($C = 14.4 Q/R$) must exceed the homolytic bond dissociation energy D_0 (in eV) of the ligand:

$$\text{EA} + 14.4 \frac{Q}{R} > D_0. \quad (2)$$

This condition allows the asymptote of the σ^* -attached state to lie below the minimum on the parent ion's surface. This makes it possible for direct attachment to the ligand antibonding orbital to occur (if the σ^* -attached surface is not too repulsive at shorter distances). However, to permit the process found to dominate here (Rydberg attachment followed by Rydberg-to- σ^* electron transfer), $\text{EA} + 14.4Q/R$ must be near or below the bottom of the Rydberg-attached state's curve:

$$\text{EA} + 14.4 Q/R \geq D_0 + \text{EA}_{\text{Rydberg}}. \quad (3)$$

here, $\text{EA}_{\text{Rydberg}}$ is the electron binding energy of the Rydberg-attached state. For the $[\text{Mg}(\text{H}_2\text{O})_n]^{2+}$ clusters studied here, the EA of OH is ca. 2 eV, D_0 is 5 eV, Q is 2, and $\text{EA}_{\text{Rydberg}}$ is 5 eV. Eq. (2) then requires $14.4Q/R$ to be 8 eV or larger, which implies R must be 3.35 Å or shorter. Clearly (see Fig. 6), the Mg–O distance (2.1 Å) of a first-shell water molecule meets this criterion, but the second- and third-shell distances do not.

The conditions put forth in Eq. (3) can offer guidance to others who study ECD in clusters consisting of a multiply charged ion surrounded by solvent molecules. In particular, to enhance the channel in which electron transfer to a solvent antibonding orbital occurs, it helps to have:

- a solvent fragment with a large EA,
- a cation with a small ionic radius [30] (so R can be small),
- a solvent with weak bonds (so D_0 is small).

At first glance, it would appear from Eq. (2) that using a cation of high charge (Q) would also help because $14.4Q/R$ would be large. However, the electron binding energy of the Rydberg-attached state ($\text{EA}_{\text{Rydberg}}$) scales as Q^2 , so one must also include this dependence when reaching conclusions.

Acknowledgements

This work has been supported by NSF Grant No. 0240387. Significant computer time provided by the Center for High Performance Computing at the University of Utah is also gratefully acknowledged. J.S. wishes to congratulate Prof. Eugen Illenberger on this occasion and remind him of the wonderful mountain bike adventure they shared in 2007 in Park City, Utah.

References

- [1] (a) R.D. Leib, W.A. Donald, M.F. Bush, J.T. O'Brien, E.R. Williams, *J. Am. Soc. Mass Spectrom.* 18 (2007) 1217;
(b) R.D. Leib, W.A. Donald, M.F. Bush, J.T. O'Brien, E.R. Williams, *J. Am. Chem. Soc.* 129 (2007) 4894.
- [2] C. Berg, M. Beyer, U. Achatz, S. Joos, G. Niedner-Schatteburg, V.E. Bondybey, *Chem. Phys.* 239 (1998) 379.
- [3] A.C. Harms, S.N. Khanna, A.B. Chen, A.W. Castleman, *J. Chem. Phys.* 100 (1994) 3540.
- [4] M. Sanekata, F. Misaizu, K. Fuke, S. Iwata, K. Hashimoto, *J. Am. Chem. Soc.* 117 (1995) 347.
- [5] J. Simons, M. Gutowski, *Chem. Rev.* 91 (1991) 669.
- [6] (a) I. Anusiewicz, J. Berdys-Kochanska, J. Simons, *J. Phys. Chem. A* 109 (2005) 5801;

- (b) I. Anusiewicz, J. Berdys-Kochanska, P. Skurski, J. Simons, *J. Phys. Chem. A* 110 (2006) 1261;
- (c) A. Sawicka, P. Skurski, R.R. Hudgins, J. Simons, *J. Phys. Chem. B* 107 (2003) 13505;
- (d) M. Sobczyk, P. Skurski, J. Simons, *Adv. Quantum Chem.* 48 (2005) 239;
- (e) A. Sawicka, J. Berdys-Kochanska, P. Skurski, J. Simons, *Int. J. Quantum Chem.* 102 (2005) 838;
- (f) I. Anusiewicz, J. Berdys, M. Sobczyk, A. Sawicka, P. Skurski, J. Simons, *J. Phys. Chem. A* 109 (2005) 250;
- (g) P. Skurski, M. Sobczyk, J. Jakowski, J. Simons, *Int. J. Mass Spectrom.* 265 (2007) 197;
- (h) M. Sobczyk, D. Neff, J. Simons, *Int. J. Mass Spectrom.* 269 (2008) 149;
- (i) M. Sobczyk, J. Simons, *Int. J. Mass Spectrom.* 253 (2006) 274;
- (j) M. Sobczyk, J. Simons, *J. Phys. Chem. B* 110 (2006) 7519.
- [7] We chose to begin our studies with the Mg^{2+} clusters rather than clusters containing Ca^{2+} to constrain the computational cost of our ab initio calculations. However, as we discuss later, our findings likely help clarify what is going on in all of the alkaline earth dication systems studied in Ref. [1].
- [8] (a) M. Gutowski, J. Simons, *J. Chem. Phys.* 93 (1990) 3874;
- (b) P. Skurski, M. Gutowski, J. Simons, *Int. J. Quantum Chem.* 80 (2000) 1024.
- [9] R.A. Kendall, T.H. Dunning Jr., R.J. Harrison, *J. Chem. Phys.* 96 (1992) 6796.
- [10] This device was first used in B. Nestmann, S.D. Peyerimhoff, *J. Phys. B* 18 (1985) 615;
- B. Nestmann, S.D. Peyerimhoff, *J. Phys. B* 18 (1985) 4309.
- [11] M.J. Frisch, G.W. Trucks, H.B. Schlegel, G.E. Scuseria, M.A. Robb, J.R. Cheeseman, J.A. Montgomery Jr., T. Vreven, K.N. Kudin, J.C. Burant, J.M. Millam, S.S. Iyengar, J. Tomasi, V. Barone, B. Mennucci, M. Cossi, G. Scalmani, N. Rega, G.A. Petersson, H. Nakatsuji, M. Hada, M. Ehara, K. Toyota, R. Fukuda, J. Hasegawa, M. Ishida, T. Nakajima, Y. Honda, O. Kitao, H. Nakai, M. Klene, X. Li, J.E. Knox, H.P. Hratchian, J.B. Cross, C. Adamo, J. Jaramillo, R. Gomperts, R.E. Stratmann, O. Yazyev, A.J. Austin, R. Cammi, C. Pomelli, J.W. Ochterski, P.Y. Ayala, K. Morokuma, G.A. Voth, P. Salvador, J.J. Dannenberg, V.G. Zakrzewski, S. Dapprich, A.D. Daniels, M.C. Strain, O. Farkas, D.K. Malick, A.D. Rabuck, K. Raghavachari, J.B. Foresman, J.V. Ortiz, Q. Cui, A.G. Baboul, S. Clifford, J. Cioslowski, B.B. Stefanov, G. Liu, A. Liashenko, P. Piskorz, I. Komaromi, R.L. Martin, D.J. Fox, T. Keith, M.A. Al-Laham, C.Y. Peng, A. Nanayakkara, M. Challacombe, P.M.W. Gill, B. Johnson, W. Chen, M.W. Wong, C. Gonzalez, J.A. Pople, Gaussian, Inc., Wallingford CT, 2004.
- [12] G. Schaftenaar, J.H. Noordik, *J. Comput.-Aided Mol. Des.* 14 (2000) 123.
- [13] These shifts are made to simulate a +2 charge (i.e., a Mg^{2+} ion) 4.7 Å or 7.5 Å away from the oxygen atom where the excess electron resides in OH^- .
- [14] D.J. Haxton, T.N. Rescigno, C.W. McCurdy, *Phys. Rev. A* 72 (2005) 022705;
- G. Seng, F. Lindler, *J. Phys. B* 9 (1976) 2539;
- A. Jain, D.G. Thompson, *J. Phys. B* 16 (1977) L347.
- [15] In Ref. [2] it was pointed out that such orbitals can be involved in binding an electron to the surface of such clusters. From our past works on ECD of positively charged peptides, we believe that the initial electron capture event occurs into an excited Rydberg orbital after which a series of radiative or radiationless relaxation steps occurs, ultimately leading to the ground-Rydberg state shown in Fig. 8.
- [16] C. Berg, U. Achatz, M. Beyer, S. Joos, G. Albert, T. Schindler, G. Niedner-Schatteburg, V.E. Bondybey, *Int. J. Mass Spectrom. Ion Process.* 167/168 (1997) 723.
- [17] F. Misaizu, K. Tsukamoto, M. Sanekata, K. Fuke, *Chem. Phys. Lett.* 188 (1992) 241.
- [18] F. Misaizu, K. Sanekata, K. Fuke, *J. Chem. Phys.* 100 (1994) 1161.
- [19] K. Fuke, F. Misaizu, M. Sanekata, K. Tsukamoto, S. Iwata, *Z. Phys. D* 26 (1993) 180.
- [20] M. Sanekata, F. Misaizu, K. Fuke, S. Iwata, K. Hashimoto, *J. Am. Chem. Soc.* 117 (1995) 747.
- [21] H. Watanabe, S. Iwata, K. Hashimoto, F. Misaizu, K. Fuke, *J. Am. Chem. Soc.* 117 (1995) 755.
- [22] M. Beyer, C. Berg, H.W. Görlitz, T. Schindler, U. Achatz, G. Gilbert, G. Niedner-Schatteburg, V.E. Bondybey, *J. Am. Chem. Soc.* 118 (1996) 7386.
- [23] For comparison, Mg^{2+} binds an electron to its 3s orbital to form Mg^+ by ca. 15 eV.
- [24] Specifically, the fact that 10–11 water molecules are boiled off upon electron attachment and knowing that the water-loss energy requirement is ca. 10 kcal/mol for charge-reduced clusters with six or more waters, gives rise to this estimate.
- [25] M. Peschke, A.T. Blades, P. Kebarle, *J. Phys. Chem. A* 102 (1998) 9978.
- [26] B.M. Reinhard, G. Niedner-Schatteburg, *J. Phys. Chem.* 118 (2003) 3571, In this paper it is shown that the recombination energies for $\text{Mg}(\text{H}_2\text{O})_n^{2+}$ clusters undergoing charge reduction to form $\text{Mg}(\text{H}_2\text{O})_n^{1+}$ are 5 eV for $6 < n < 20$, so our assumption is probably valid.
- [27] Our earlier studies showed that the character of this Rydberg orbital persists even if second-shell solvent molecules are present. So, although the present study involves only the six first-shell waters, we expect the conclusions drawn to be pertinent to clusters having one or more second-shell waters as well.
- [28] We had difficulty converging the Hartree–Fock orbital optimization process for the Rydberg-attached state beyond 1.3 Å, so the points shown as open squares were obtained by subtracting the (essentially constant) 5 eV energy spacing between the parent and Rydberg-attached states from the energy of the parent at these longer bond lengths.

[29] We use the relaxed σ^* -curve to reach this conclusion because we assume this process will occur after the ca. 5 eV released in the electron capture event has been randomized among the cluster's vibrational modes. Because the geometry of the Rydberg-attached state does not undergo much geometrical change upon electron attachment, we assume that the Rydberg-state curve shown in

Fig. 10 (which has the cluster at the parent's geometry) is equally valid for the geometry-relaxed Rydberg state.

[30] The ionic radii of alkaline earth dications range from 0.41 Å and 0.86 Å for Be and Mg to 1.49 Å for Ba.